LI-RADS: Diagnostic Performance of Hepatobiliary Phase Hypointensity and Major Imaging Features of LR-3 and LR-4 Lesions Measuring 10–19 mm With Arterial Phase Hyperenhancement

Federica Vernuccio[1,2]
Roberto Cannella[3,4]
Mathias Meyer[1]
Kingshuk Roy Choudhoury[5]
Fernando Gonzáles[1,6]
Fides R. Schwartz[1]
Rajan T. Gupta[1]
Mustafa R. Bashir[1,7]
Alessandro Furlan[3]
Daniele Marin[1]

Keywords: gadoxetate disodium, gadoxetic acid, cirrhosis, hepatocellular carcinoma, liver, MRI, sensitivity, specificity

doi.org/10.2214/AJR.18.20979

F. Vernuccio and R. Cannella contributed equally to this study.

Received December 3, 2018; accepted after revision February 9, 2019.

[1]Department of Radiology, Duke University Medical Center, 2301 Erwin Rd, Durham, NC 27710. Address correspondence to D. Marin (daniele.marin@duke.edu).

[2]Promozione della Salute, Materno-Infantile, di Medicina Interna e Specialistica di Eccellenza G. D'Alessandro, University of Palermo, Palermo, Italy.

[3]Department of Radiology, University of Pittsburgh Medical Center, Pittsburgh, PA.

[4]Department of Biopathology and Medical Biotechnologies, University of Palermo, Palermo, Italy.

[5]Department of Biostatistics and Bioinformatics, Duke University School of Medicine, Durham, NC.

[6]Department of Radiology, Clínica Alemana de Santiago, Universidad del Desarrollo, Santiago, Chile.

[7]Center for Advanced Magnetic Resonance Development and Department of Medicine, Duke University, Durham, NC.

WEB
This is a web exclusive article.

Supplemental Data
Available online at www.ajronline.org.

AJR 2019; 213:W57–W65

0361–803X/19/2132–W57

OBJECTIVE. The purpose of this study was to determine the diagnostic performance of hepatobiliary phase hypointensity and Liver Imaging Reporting and Data System (LI-RADS) major imaging features in the diagnosis of hepatocellular carcinoma (HCC) in hepatic lesions with arterial phase hyperenhancement (APHE) measuring 10–19 mm in patients at high risk of HCC.

MATERIALS AND METHODS. A composite reference standard of pathologic analysis and imaging follow-up was used. The diagnostic performance (sensitivity and specificity) of hepatobiliary phase hypointensity and LI-RADS major imaging features other than APHE for the diagnosis of HCC was assessed and compared by means of a logistic regression model.

RESULTS. This retrospective dual-institution study included 189 LI-RADS LR-3 and LR-4 lesions measuring 10–19 mm and having APHE in 144 consecutively registered patients (96 men, 48 women; mean age, 58 years). Hepatobiliary phase hypointensity had significantly higher sensitivity (84% [92/109], $p < 0.00001$) than major imaging features in the diagnosis of HCC but lower specificity (84% [67/80]; $p = 0.01$). However, hepatobiliary phase hypointensity in LR-3 observations measuring 10–19 mm and having APHE had moderately elevated sensitivity (73% [44/60]) and specificity (85%, 64/75). All three major imaging features had high specificity for the diagnosis of HCC, including 95% (76/80) for washout, 100% (80/80) for enhancing capsule, and 99% (79/80) for threshold growth.

CONCLUSION. Major imaging features have high specificity for the diagnosis of HCC in lesions measuring 10–19 mm that have APHE. The finding of hepatobiliary phase hypointensity significantly improves sensitivity while moderately high specificity is maintained for the diagnosis of HCC in LR-3 lesions measuring 10–19 mm that exhibit APHE.

The Liver Imaging Reporting and Data System (LI-RADS) endorsed by the American College of Radiology stratifies liver lesions in patients at high risk of hepatocellular carcinoma (HCC) into different categories reflecting their relative probability of being benign, HCC, or other hepatic malignant neoplasms [1]. Although LI-RADS has had high diagnostic performance in the characterization of lesions 20 mm and larger [2–4], major diagnostic challenges—with a potential failure rate of 87%—remain in the assessment of lesions measuring 10–19 mm that have arterial phase hyperenhancement (APHE) [5, 6]. This poses a serious clinical problem because these lesions are highly prevalent and difficult to diagnose definitively as HCC or benign and because early diagnosis of HCC is critical for improving patient survival [7].

Prior studies [8–10] have shown that MRI with hepatobiliary contrast agents may have significantly higher sensitivity than multiphasic CT and MRI with extracellular agents in the diagnosis of HCC in lesions measuring 10–19 mm. Unfortunately, along with improved sensitivity, use of hepatobiliary MRI contrast agents may also result in lower specificity, mainly owing to inability to differentiate HCC from other liver lesions, including benign entities (e.g., hemangiomas, nodular or confluent areas of fibrosis, siderotic nodules) and non-HCC malignancies (e.g., intrahepatic cholangiocarcinoma, metastases) [8–13]. Preserving high specificity for the diagnosis of HCC has important clinical implications, such as preventing unnecessary treatment of benign lesions and avoiding misallocation of transplant livers due to the different prognoses of HCC and non-HCC malignancy [11]. Because of the detrimental effect of lower

specificity on appropriate organ allocation to liver transplant candidates, most U.S. and European HCC diagnostic algorithms have not incorporated hepatobiliary MRI contrast agents as a first-line method in the diagnosis and staging of HCC [1, 11, 14]. This is also the reason that hepatobiliary phase hypointensity is regarded as an ancillary feature rather than a major imaging feature in the diagnosis of HCC by means of LI-RADS.

Several limitations may have negatively affected the results of prior studies of the diagnostic performance of hepatobiliary phase imaging in the diagnosis of HCC. For example, most studies rely on results from only a single institution, are confounded by both selection and misclassification biases [15], include the transitional phase for characterizing major imaging features of HCC (e.g., washout and capsule appearances), and do not differentiate lesions suggestive of malignancies other than HCC (i.e., those with rim APHE or peripheral washout). These approaches may have unduly decreased the specificity of hepatobiliary contrast agents for the diagnosis of HCC.

We hypothesize that larger multicenter clinical studies designed to overcome some of the limitations of prior investigations and focused on challenging hepatic lesions with APHE may show improved specificity of MRI with hepatobiliary contrast agents for the diagnosis of HCC with the LI-RADS lexicon. The purpose of this dual-institution study was to determine the diagnostic performance of hepatobiliary phase hypointensity and LI-RADS major imaging features for the diagnosis of HCC in hepatic lesions measuring 10–19 mm with APHE in patients at high risk of HCC.

Materials and Methods

This retrospective, dual-institution, HIPAA-compliant study received institutional review board approval, and waivers of the requirement for informed consent were obtained. The two study institutions (Duke University, University of Pittsburgh) are referral centers for patients with liver disease, and each perform more than 80 liver transplants per year. The authors had control of the data and the information submitted for publication. There was no industry support for this study.

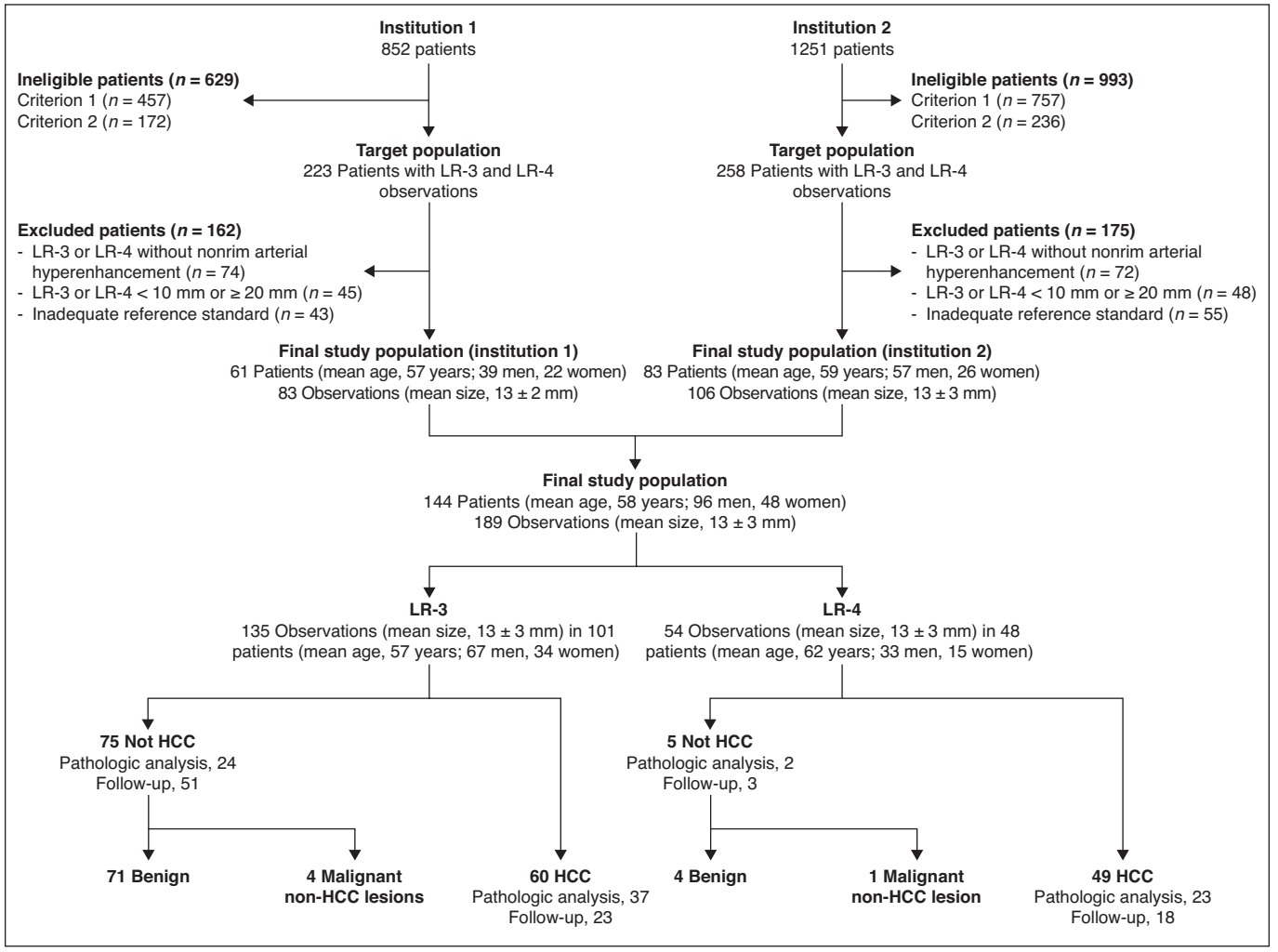

Fig. 1—Flowchart shows study enrollment based on recommended Standards for Reporting of Diagnostic Performance criteria and on reference standard. Enrollment began with database search at two institutions of records of 2103 patients at high risk of hepatocellular carcinoma (HCC) with at least one gadoxetate disodium–enhanced MRI examination. Criterion 1 = no liver observations, only benign or probably benign observations (Liver Imaging Reporting and Data System version 2017 [LR] category 1 and 2) or observations that could not be categorized owing to image degradation of omission (LR-NC). Criterion 2 = only lesions categorized as definitely HCC (LR-5, LR-5g, and LR-5us), definite tumor in vein (LR-TIV), treated observation (LR-TR), or probably or definitely malignant but not HCC specific (LR-M).

Study Cohort

Figure 1 shows the subject accrual flowchart, which followed the Strengthening the Reporting of Observational Studies in Epidemiology initiative guidelines [16]. We retrospectively searched the departmental electronic databases at our tertiary academic institutions for consecutively registered patients at high risk of development of HCC according to LI-RADS who underwent liver MRI with a commercially available hepatobiliary contrast agent (gadoxetate disodium, Eovist, Bayer HealthCare) between January 1, 2009, and December 31, 2014. During this study time frame, gadoxetate disodium was the standard of care for HCC screening at both institutions.

The initial search yielded the records of 2103 patients at high risk of HCC with applicable MRI examinations. Patients were then excluded if they met any of the following criteria on the basis of review of available MRI reports and imaging analysis of the lesions: no liver lesion or only definitely benign or probably benign lesions (categories LR-1 and LR-2) (n = 1174); only lesions consistent with definite HCC (LR-5, LR-5g, and LR-5us), tumor in vein (LR-TIV), treated lesions (LR-TR), or probably or definitely malignant but not HCC specific (LR-M) (n = 408). In 40 patients, lesions could not be categorized because of image degradation or omission (LR-NC).

The search yielded a target population of 481 consecutive patients who were deemed eligible for inclusion in the study. In eligible patients, lesions were further excluded on the basis of the following criteria: size smaller than 10 mm or larger than 19 mm; absence of nonrim APHE, categorization as definite HCC (i.e., LR-5, LR-5g, or LR-5us), and inadequate reference standard (see later, Reference Standards, and Appendix 1). Categorization as definite HCC, according to LI-RADS version 2017, included the presence of two or more major imaging features apart from nonrim APHE (i.e., LR-5), presence of nonperipheral washout and visibility at screening ultrasound (LR-5us) or 50% or greater diameter increase in less than 6 months (LR-5g). By application of these exclusion criteria, only LR-3 and LR-4 lesions with APHE, measuring 10–19 mm, and having only one additional major feature were included in this study. The presence of only a major feature in addition to APHE was not an exclusion criterion because these lesions measuring 10–19 mm could not reach the LR-5 category according to LI-RADS version 2017.

Using the electronic data repository systems at both institutions, we collected patient-related variables, including sex, age, Child-Pugh score [17, 18], Model for End-Stage Liver Disease score combined with sodium concentration (MELDNa) [19], and albumin-bilirubin score [20].

MRI Technique

Dynamic contrast-enhanced liver MRI examinations had been performed with seven different clinical MRI systems of four different types, including both 1.5-T and 3-T systems. Detailed pulse sequence parameters are listed in Table S1. (Tables S1 and S2 and Fig. S3 can be viewed in the *AJR* electronic supplement to this article, available at www.ajronline.org.) Given the dual-institution retrospective nature of this study, various MRI systems were used, but all of the MRI examinations were performed with comparable, clinically appropriate liver protocols [21], which included unenhanced, single-breath-hold, T2-weighted 2D turbo spin-echo and T1-weighted 2D dual gradient-recalled echo MRI. After unenhanced imaging, patients received a weight-based dose of 0.025 mmol/kg of gadoxetate disodium (Eovist, Bayer HealthCare) injected with a power injector at a rate of 1–2 mL/s. Contrast administration was followed by a 20-mL 0.9% saline flush at the same injection rate. T1-weighted 3D spoiled gradient-recalled echo breath-hold images were obtained after contrast injection during the late hepatic arterial, portal venous, and transitional phases and during the liver-specific hepatobiliary phase (20 minutes after contrast administration). The optimal imaging delay for the late hepatic arterial phase was determined with a single-breath-hold triple arterial phase protocol or a single late arterial phase acquisition [21–23].

MRI Analysis

Two radiologists with expertise in abdominal imaging reviewed the MRI examinations at each institution in consensus at the same time using a clinical PACS (Centricity 4.2, GE Healthcare; iSite PACS, Philips Healthcare). The radiologists were aware of the purpose and design of the study, but they were blinded to patient demographics, clinical history, clinical report, and reference standard.

For each lesion, the readers documented the presence of three major imaging features according to LI-RADS version 2017 [1]: nonperipheral washout in the portal venous phase, enhancing capsule in either the portal venous or transitional phase, and threshold growth. These major imaging features are defined in Appendix 1. On the basis of analysis of major features only, lesions were categorized as LR-3 if no additional major features were present besides nonrim APHE; LR-4 if only one of the following additional major features was present: nonperipheral washout, enhancing capsule, or threshold growth, defined as 100% or greater increase in size in more than 6 months or previously unseen lesion and now growing 10 mm or more in 24 months or less. LR-4 APHE lesions with 50% or greater increase in diameter in less than 6 months were categorized as LR-5g according to LI-RADS version 2017. Therefore, they were considered ineligible according to our exclusion criteria. Increase in size or growth of the lesions less than the aforementioned definitions—defined as subthreshold growth—was not assessed in our study. To mitigate the potential confounding effect of assessing multiple lesions in the same patient (i.e., clustering bias [17]), a maximum of three lesions per category (LR-3 and LR-4) were assessed in each patient.

In addition to the aforementioned major imaging features, the readers also documented the presence or absence of hepatobiliary phase hypointensity—defined as intensity in the hepatobiliary phase unequivocally less, in whole or in part, than that of liver—which is currently regarded as one of the ancillary imaging features favoring malignancy, not HCC in particular, according to LI-RADS. We did not assess transitional phase hypointensity—a different ancillary feature in the LI-RADS lexicon—in our study because there are only scant data about its added value for the diagnosis of HCC, and owing to our retrospective dual-institution study design, there was no standardization of the time for acquisition in transitional phases.

Reference Standard

The reference standard was established by one radiology fellow at each institution. These fellows had access to electronic patient medical records, including pathology reports and all images obtained before and after the index examination, and reviewed all serial images obtained before and after the index examination for evaluation of final LI-RADS categorization of each lesion.

A composite reference standard of pathologic and imaging follow-up was used to establish ultimate diagnosis, including malignancy or benignancy (Appendix 1). The diagnosis of HCC required pathologic proof of HCC or untreated lesion with conclusive criteria for the diagnosis of definitive HCC at imaging follow-up (i.e., lesion meeting the criteria for LR-5, LR-5us, or LR5-g). To minimize the potential confounding effect of misclassification bias (i.e., inappropriate inclusion of premalignant lesions at baseline, such as dysplastic nodules, due to the delay between imaging and the final diagnosis of HCC), a maximum interval of 12 months was allowed between the index MRI examination and the date of HCC confirmation with the reference standard [4].

The benign nature of the lesions was based on either pathologic proof at any time or stability or resolution at imaging follow-up with CT or MRI for a minimum of 24 months. This interval time matches the LI-RADS version 2017 definition of

size stability, which is an ancillary feature favoring benignancy [1].

Statistical Analysis

Data were summarized as counts and percentages for categoric variables and by mean and SD and range or as median and interquartile range for continuous variables. Categoric and continuous variables were compared by Fisher exact test or chi-square test and *t* test as appropriate.

The diagnostic performance in the diagnosis of HCC in the lesions of interest (measuring 10–19 mm with APHE) was determined and compared between the two institutions as follows: performance of each major imaging feature (except APHE, which was present in all lesions of interest) and performance of hepatobiliary phase hypointensity, assessed separately for the LR-3 and LR-4 lesions.

According to the Bayes theorem, positive and negative predictive values were not calculated because these values directly depend on the prevalence of the finding in the population being tested and might be not indicative of the findings that might be observed in other settings

In the assessment of diagnostic performance, a result was regarded as true-positive when an imaging diagnosis of HCC was made and was confirmed with the reference standard, false-positive when an imaging diagnosis of HCC was made but a non-HCC diagnosis was made with the reference standard, false-negative when an imaging diagnosis of HCC was not made but the reference standard was diagnostic of HCC, and true-negative when an imaging diagnosis of HCC was not made but HCC was confirmed with the reference standard.

Sensitivity and specificity of individual imaging features were compared by fitting a model of the form

$$\log \frac{p_{ij}}{1-p_{ij}} = \mu + \alpha_j + b_i$$

where p_{ij} is the probability of detection for the i-th HCC lesion ($i = 1, \ldots, 189$) by use of the j-th imaging feature (j is nonperipheral washout, enhancing capsule, threshold growth, or hepatobiliary phase hypointensity). In the model, μ represents the baseline log-odds for detection (baseline marker is nonperipheral washout), α_j is the effect of the j-th marker, that is, difference from baseline, and b_i is the effect of the i-th lesion, which is assumed to be random with a zero mean gaussian distribution. The model was fit by restricted maximum likelihood by use of the lme4 package in the R computing platform (version 3.4.3, R Project). Enhancing capsule was not included in this analysis because its specificity was 100%, leading to infinite odds (1/0). For each analysis, $p < 0.05$ was considered statistically significant. All statistical tests were two sided. Missing data were excluded from the analysis. All statistical analyses were performed with the R computing platform (version 3.4.3, R Project).

Results

Our final study population consisted of 144 patients (mean age, 58 ± 10 years; range 20–81 years; 96 men [mean age, 59 ± 9 years; range, 31–81 years], 48 women [mean age, 57 ± 13 years; range, 20–80 years]) (Fig. 1). Characteristics of the study population at each institution are summarized in Table S2. A total of 189 lesions (mean diameter, 13 ± 3 mm; range, 10–19 mm) were included in the study, including a single lesion in 108 patients (mean diameter, 13 ± 3 mm; range, 10–19 mm), two lesions in 28 patients (13 ± 2 mm; range, 10–19 mm), three lesions in seven patients (13 ± 3 mm; range, 10–17 mm]), and four lesions in one patient (including two category LR-3 and two LR-4, 14 ± 3 mm; range, 11–18 mm). Of these 189 lesions, 135 (71%) were categorized LR-3 (13 ± 3 mm; range, 10–19 mm) because of lack of additional major imaging features other than APHE. Fifty-four (29%) lesions were categorized LR-4 (mean diameter, 13 ± 3 mm; range, 10–19 mm) on the basis of nonperipheral washout in 34 lesions (63%), enhancing capsule in eight (15%), and threshold growth in 12 (22%). Of note, 109 of the 189 lesions were diagnosed as HCC with the reference standard, including 60 lesions categorized LR-3 and 49 lesions categorized LR-4.

All three major imaging features had high specificity for the diagnosis of HCC: 95% (76/80; 95% CI, 87–99%) for washout, 100% (80/80) for enhancing capsule, and 99% (79/80; 95% CI, 93–100%) for threshold growth (Table 1 and Fig. 2). Low sensitivity values were observed for all major imaging features, ranging from 7% (8/109; 95% CI, 3–14%) for enhancing capsule to 28% (30/109; 95% CI, 19–37%) for washout (Table 1 and Fig. 3). Compared with the major imaging features, hepatobiliary phase hypointensity had significantly higher sensitivity (84% [92/109]; 95% CI, 76–91%; $p <$ 0.00001) for the diagnosis of HCC with an odds ratio of 15.03 (Fig. 3 and Table 2). This improvement in sensitivity, however, came at the cost of significantly lower specifici-

TABLE 1: Diagnostic Performance of Major Imaging Features and Hepatobiliary Phase Hypointensity in Diagnosis of Hepatocellular Carcinoma (HCC) by Institution

Imaging Feature	Sensitivity (%)[a]		Specificity (%)[b]	
	Value	95% CI	Value	95% CI
Entire study population				
Nonperipheral washout	28 (30/109)	19–37	95 (76/80)	87–99
Enhancing capsule	7 (8/109)	3–14	100 (80/80)	
Threshold growth[c]	10 (11/109)	5–17	99 (79/80)	93–100
Hepatobiliary phase hypointensity	84 (92/109)	76–91	84 (67/80)	74–91
Institution 1				
Nonperipheral washout	35 (11/31)	19–55	94 (49/52)	84–99
Enhancing capsule	10 (3/31)	2–26	100 (52/52)	90–100
Threshold growth[c]	0 (0/31)		98 (51/52)	
Hepatobiliary phase hypointensity	84 (26/31)	66–95	90 (47/52)	79–97
Institution 2				
Nonperipheral washout	24 (19/78)	15–35	96 (27/28)	82–100
Enhancing capsule	6 (5/78)	2–14	100 (28/28)	
Threshold growth[c]	14 (11/78)	7–24	100 (28/28)	
Hepatobiliary phase hypointensity	85 (66/78)	75–92	71 (20/28)	51–87

Note—No significant differences in sensitivity or specificity were observed between the two institutions for any imaging feature ($p > 0.06$).

[a]Values in parentheses are number of HCCs.

[b]Values in parentheses are number of lesions not HCCs.

[c]Threshold growth based on 100% or greater increase in size in more than 6 months or previously unseen and now 10 mm or greater in 24 months or less.

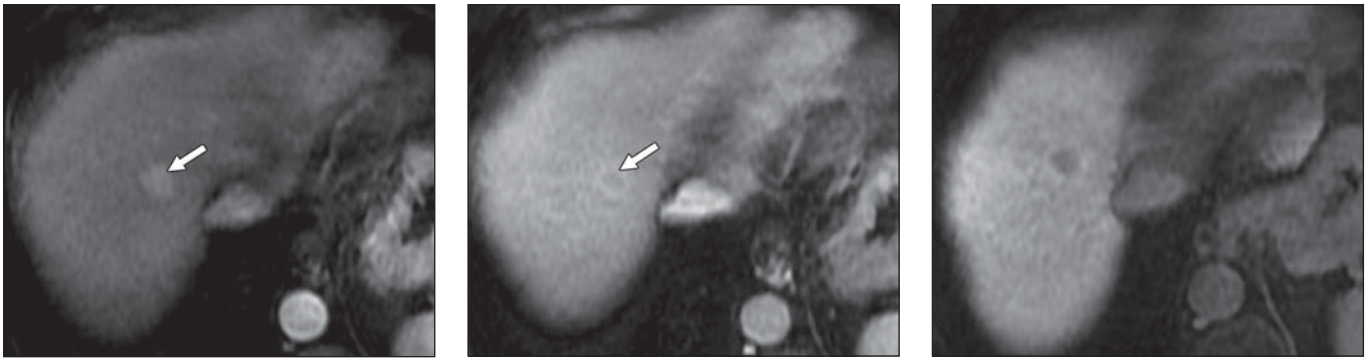

Fig. 2—71-year-old man with alcohol-related cirrhosis and observation categorized as Liver Imaging Reporting and Data System version 2017 LR-4 according to major imaging features. Pathologic specimen was obtained during laparoscopic ablation of lesion 6 months after this imaging examination. Final diagnosis at pathologic analysis was hepatocellular carcinoma (HCC). In this LR-4 lesion measuring 14 mm, presence of enhancing capsule in addition to arterial phase hyperenhancement (not rim) should be considered sufficient for diagnosis of HCC.
A, Gadoxetate disodium–enhanced MR image shows 14-mm lesion (*arrow*) with arterial phase hyperenhancement (not rim) (lack of nonperipheral washout).
B, Portal venous phase image shows evidence of enhancing capsule (*arrow*).
C, Hepatobiliary phase image shows hypointensity.

ty (84% [67/80]; 95% CI, 74–91%; $p = 0.01$ for all comparisons) due to 13 false-positive findings in the hepatobiliary phase, including three combined HCC-cholangiocarcinomas (Fig. S3), one angiomyolipoma, one macroregenerative nodule with fatty infiltration (Fig. 4), and eight benign lesions, which were proved benign on the basis of stability for a minimum of 24 months ($n = 5$) or resolution at follow-up with CT or MRI ($n = 3$).

The diagnostic performance of hepatobiliary phase hypointensity in the diagnosis of HCC was substantially different between LR-3 and LR-4 lesions. For LR-4 lesions, hepatobiliary phase hypointensity had nearly perfect sensitivity (98% [48/49]; 95% CI, 89–100%]) but substantially lower specificity (60% [3/5]; 95% CI, 15–95%) (Figs. 4 and S3 and Table 3). Conversely, the sensitivity was lower (73% [44/60]; 95% CI, 60–84%]) and specificity higher (85% [64/75]; 95% CI, 75–92%]) for hepatobiliary phase hypointensity in the subset of LR-3 lesions (Fig. 3 and Table 3).

Discussion

Our results showed that compared with current LI-RADS major imaging features, the finding of hepatobiliary phase hypointensity improves sensitivity in the diagnosis of HCC in APHE lesions measuring 10–19 mm (odds ratio, 15.03; $p < 0.00001$). The result likely reflects reduced expression of organic anion transporting polypeptide 1B1/3 (OATP1B/3), which leads to decreased uptake of the hepatobiliary contrast agent into the lesion and hypointensity on hepatobiliary phase images, a hepatocarcinogenic step that may precede the occurrence of washout in small early or progressed HCCs [24]. In our study, assessment of hepatobiliary phase hypointensity led to identification of 73% (44/60) of HCCs in lesions with intermediate probability of malignancy (i.e., category LR-3), which poses a common diagnostic conundrum.

Our data showed a significant decrease in specificity for hepatobiliary phase hypointensity compared with major imaging features, which is in agreement with previous literature [8, 10, 12, 13]. In our study, however, the specificity of hepatobiliary phase hypointensity remained high (85% [64/75]; 95% CI, 75–92%) for the subset of LR-3 lesions ($n = 135$) lacking major features besides APHE. This specificity level compares favorably with that of washout appearance for similar observations in a recent study [24]. Our results may provide preliminary evidence to justify the use of hepatobiliary phase hypointensity for mandatory upgrade to LR-4 of all LR-3 lesions measuring 10–19 mm that have APHE. The proposed change

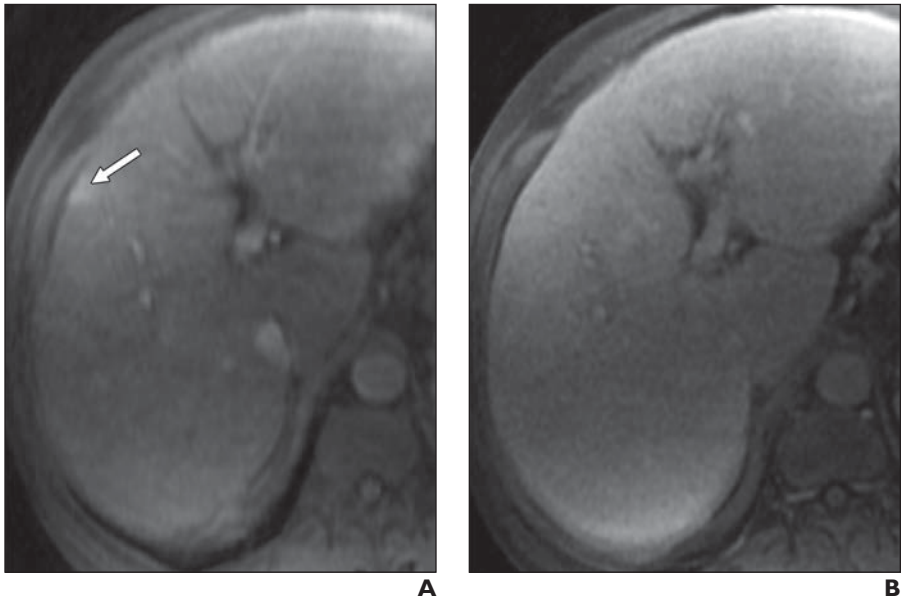

Fig. 3—59-year-old man with hepatitis B virus cirrhosis and observation categorized as Liver Imaging Reporting and Data System version 2017 LR-3 according to major imaging features.
A, Arterial phase gadoxetate disodium–enhanced MR image shows 10-mm lesion (*arrow*) with hyperenhancement (not rim).
B, Portal venous phase image shows lack of nonperipheral washout or enhancing capsule.

(Fig. 3 continues on next page)

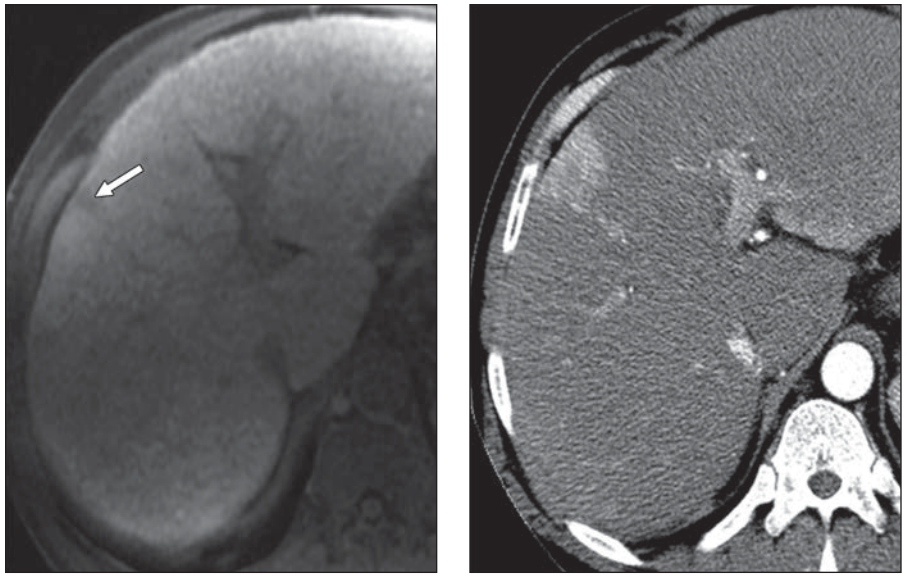

C D

Fig. 3 (continued)—59-year-old man with hepatitis B virus cirrhosis and observation categorized as Liver Imaging Reporting and Data System version 2017 LR-3 according to major imaging features.
C, Hepatobiliary phase image shows hypointensity (*arrow*).
D, Four-month follow-up CT image shows lesion upgraded to LR-5 (size ≥ 20 mm, arterial phase hyperenhancement, and threshold growth).

TABLE 2: Logistic Regression Models Comparing Diagnostic Performance Across Imaging Features

Imaging Feature	Log Odds	Odds	SE	*z*	*p*
Model for sensitivity					
Baseline; nonperipheral washout	−0.99	0.37	0.24	−4.18	
Enhancing capsule	−1.58	0.21	0.43	−3.65	0.0003
Hepatobiliary phase	2.71	15.03	0.41	6.59	< 0.00001
Hypointensity					
Threshold growth[a]	−1.23	0.29	0.39	−3.15	0.002
Model for specificity					
Baseline: nonperipheral washout	10.08	23,860.99	2.5	4.03	
Hepatobiliary phase	−3.65	0.03	1.37	−2.66	0.01
Hypointensity					
Threshold growth[a]	2.12	8.33	1.46	1.45	0.15

Note—Baseline for these models is lesions with nonperipheral washout. Enhancing capsule was not included in the model for specificity because its specificity of 100% led to infinite odds (1/0). SE = standard error.
[a]Threshold growth based on 100% or greater increase in size in more than 6 months or previously unseen and now 10 mm or greater in 24 months or less.

in the current diagnostic algorithm may have important clinical implications, resulting in more aggressive management (such as biopsy or decreasing the imaging follow-up interval) of these clinically challenging lesions.

Our study showed that 93% of lesions categorized LR-4 with LI-RADS version 2017 are HCC, the specificity of current major imaging features being nearly perfect (> 95%) for the diagnosis of HCC in APHE lesions measuring 10–19 mm. Our data corroborate the results of prior studies showing specificity between 89% and 99% for the combination of APHE in conjunction with nonperipheral washout or capsule appearance for the diagnosis of HCC [4, 8, 11]. This accumulating literature supports the modifications made in LI-RADS version 2018 [11, 25], which call for use of a single major imaging feature (either nonperipheral washout or tumor growth) for the confirmatory diagnosis of HCC (i.e., LR-5) in APHE lesions larger than 10 mm. Rapid implementation of these new guidelines is important to enable earlier diagnosis of HCC, decrease the time from diagnosis to treatment, decrease the number of unnecessary diagnostic biopsies and follow-up examinations, and improve patient outcomes.

Our study showed higher specificity of capsule appearance compared with both nonperipheral washout and threshold growth for the diagnosis of HCC in APHE lesions measuring 10–19 mm. In accordance with other observations [24, 26, 27], our results indicate that capsule appearance is a highly specific imaging feature of HCC, and though less commonly present, it may be comparable to nonperipheral washout and threshold growth for the diagnosis of HCC in APHE lesions larger than 10 mm. By upgrading LR-4 APHE lesions measuring 10–19 mm to LR-5, sensitivity for the diagnosis of HCC would be significantly improved. Therefore, enhancing capsule may be considered a major feature for categorizing APHE lesions larger than 10 mm as LR-5.

Limitations

In addition to its retrospective design, several limitations of our study deserve attention. First, we did not have pathologic proof in 40% (44/109) of lesions, which proved to be HCC at imaging follow-up. Although this approach has been widely adopted in previous studies because it reflects routine practice in guiding clinical decisions for patients at risk of HCC (including potential liver transplant candidates), this approach may have led to incorporation bias, and we cannot entirely rule out the possibility of misdiagnosis in a small number (≈ 5%) of lesions categorized as LR-5 at imaging follow-up [24].

Second, the specificity of hepatobiliary phase hypointensity was only 60% (95% CI, 15–95%) for the diagnosis of HCC in LR-4 lesions. Caution is warranted in the interpretation of this finding because of the very low number (n = 5) of non-HCC lesions in the subset of LR-4 lesions, which may have significantly skewed our results. Future studies in larger patient cohorts are warranted to validate our preliminary results.

Third, we analyzed only hepatobiliary phase hypointensity, excluding analysis of the presence of other ancillary features. We used this approach because hepatobiliary phase hypointensity is reported in 79–99% of

TABLE 3: Diagnostic Performance of Hepatobiliary Phase Hypointensity in Liver Imaging Reporting and Data System Category LR-3 and LR-4 Lesions by Institution

Population	LR-3		LR-4	
	Value	95% CI	Value	95% CI
Total				
Sensitivity[a]	73 (44/60)	60–84	98 (48/49)	89–100
Specificity[b]	85 (64/75)	75–92	60 (3/5)	15–95[c]
Institution 1				
Sensitivity[a]	71 (12/17)	44–90	100 (14/14)	
Specificity[b]	92 (44/48)	80–98	75 (3/4)	19–99[c]
Institution 2				
Sensitivity[a]	74 (32/43)	59–86	97 (34/35)	85–100
Specificity[b]	74 (20/27)	54–89	0 (0/1)[c]	

[a]Values in parentheses are number of hepatocellular carcinomas (HCCs).
[b]Values in parentheses are numbers of lesions not HCC.
[c]There were too few cases of LR-4 lesions that turned out to be not HCC (i.e., benign or malignant other than HCC) for accurate analysis of specificity.

HCCs and its incorporation as a key diagnostic feature is highly debated in the radiologic literature, whereas other ancillary features occur less frequently [9, 24, 28]. In addition, the MRI techniques were not strictly consistent with LI-RADS imaging guidelines, owing to thicker slices for some dynamic images. Furthermore, because these are older cases, the technology and image quality may not be representative of newer MRI systems, separate from compliance with the minimal LI-RADS imaging guidelines.

Fourth, the imaging analysis was performed in consensus, and we did not calculate interreader agreement. Although this may have introduced evaluation bias, other investigators [29] had already reported high agreement for characterization of major features. Our rationale was to provide reliable results on hepatobiliary phase hypointensity.

Finally, it is conceivable that our reported low sensitivity of the major imaging features for the diagnosis of HCC may be partially related to the evaluation of nonperipheral washout during the portal venous phase only, owing to the lack of conventional delayed phase imaging with gadoxetate disodium [21]. Prior evidence on conventional extracellular contrast agents indicates superior diagnostic performance of delayed phase compared with portal venous phase imaging for the detection of washout and capsule [30].

Conclusion

Our data suggest that the finding of hepatobiliary phase hypointensity significantly improves sensitivity for the diagnosis of HCC in APHE lesions measuring 10–19 mm while maintaining moderately high specificity for lesions with intermediate probability of malignancy (i.e., LR-3). Our data also showed nearly perfect specificity of all LI-RADS major imaging features, which supports the recently revised clinical practice recommendations for single major imaging feature (i.e., nonperipheral washout or tumor growth) for the definitive diagnosis of HCC in APHE lesions larger than 10 mm.

Acknowledgment

We thank Sheela Agarwal for help in manuscript revision.

References

1. American College of Radiology website. CT/MRI LI-RADS® v2017 core. www.acr.org/-/media/ACR/Files/RADS/LI-RADS/LIRADS_2017_Core.pdf?la=en. Accessed April 23, 2018
2. Bolondi L, Gaiani S, Celli N, et al. Characterization of small nodules in cirrhosis by assessment of vascularity: the problem of hypovascular hepatocellular carcinoma. *Hepatology* 2005; 42:27–34
3. Chou R, Cuevas C, Fu R, et al. Imaging techniques for the diagnosis of hepatocellular carci-

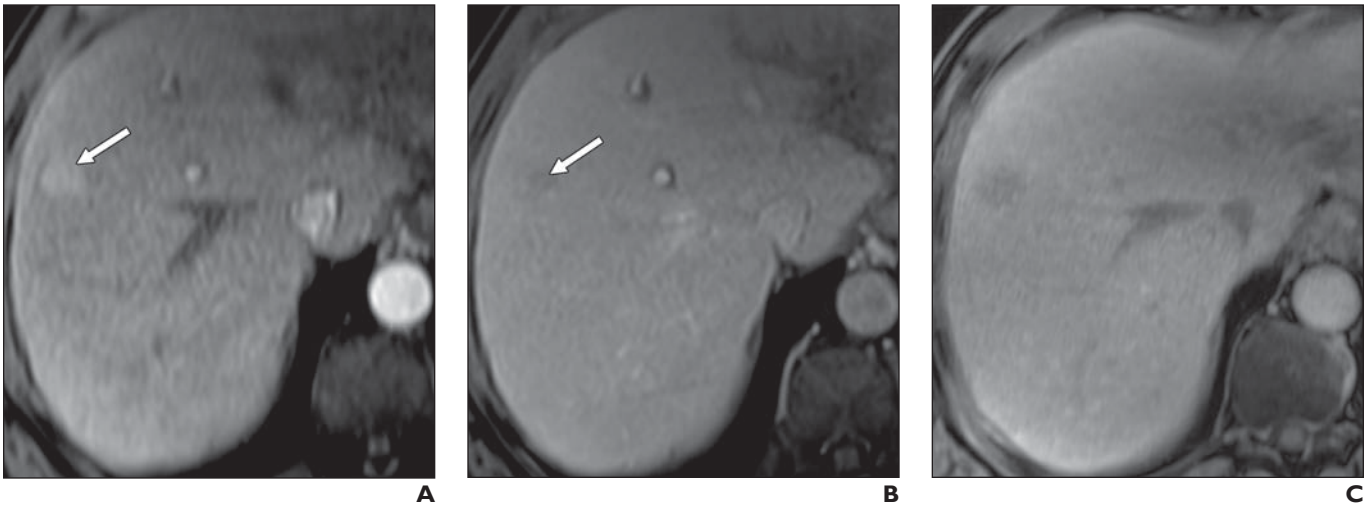

Fig. 4—57–year-old man with hepatitis C virus cirrhosis and observation categorized as Liver Imaging Reporting and Data System version 2017 LR-4 according to major imaging features. Patient underwent surgical resection 4 months after imaging with final diagnosis of macroregenerative nodule with severe (40–50%) fatty infiltration.
A, Arterial phase gadoxetate disodium–enhanced MR image shows 12-mm lesion (*arrow*) with hyperenhancement (not rim).
B, Portal venous phase image shows nonperipheral washout (*arrow*).
C, Hepatobiliary phase image shows hypointense area.

noma: a systematic review and meta-analysis. *Ann Intern Med* 2015; 162:697–711

4. Tang A, Bashir MR, Corwin MT, et al.; LI-RADS Evidence Working Group. Evidence supporting LI-RADS major features for CT- and MR imaging-based diagnosis of hepatocellular carcinoma: a systematic review. *Radiology* 2018; 286:29–48
5. Furlan A, Borhani AA. Problematic lesions in cirrhosis. *Clin Liver Dis (Hoboken)* 2018; 11:43–47
6. Holland AE, Hecht EM, Hahn WY, et al. Importance of small (≤ 20-mm) enhancing lesions seen only during the hepatic arterial phase at MR imaging of the cirrhotic liver: evaluation and comparison with whole explanted liver. *Radiology* 2005; 237:938–944
7. Tanabe M, Kanki A, Wolfson T, et al. Imaging outcomes of liver imaging reporting and data system version 2014 category 2, 3, and 4 observations detected at CT and MR imaging. *Radiology* 2016; 281:129–139
8. Roberts LR, Sirlin CB, Zaiem F, et al. Imaging for the diagnosis of hepatocellular carcinoma: a systematic review and meta-analysis. *Hepatology* 2018; 67:401–421
9. Renzulli M, Biselli M, Brocchi S, et al. New hallmark of hepatocellular carcinoma, early hepatocellular carcinoma and high-grade dysplastic nodules on Gd-EOB-DTPA MRI in patients with cirrhosis: a new diagnostic algorithm. *Gut* 2018; 67:1674–1682
10. Choi SH, Lee SS, Park SH, et al. LI-RADS classification and prognosis of primary liver cancers at gadoxetic acid–enhanced MRI. *Radiology* 2018; 290:388–397
11. Marrero JA, Kulik LM, Sirlin CB, et al. Diagnosis, staging, and management of hepatocellular carcinoma: 2018 practice guidance by the American Association for the Study of Liver Diseases. *Hepatology* 2018; 68:723–750
12. Choi SH, Lee SS, Kim SY, et al. Intrahepatic cholangiocarcinoma in patients with cirrhosis: differentiation from hepatocellular carcinoma by using gadoxetic acid-enhanced MR imaging and dynamic CT. *Radiology* 2017; 282:771–781
13. Lee MH, Kim SH, Park MJ, Park CK, Rhim H. Gadoxetic acid-enhanced hepatobiliary phase MRI and high-b-value diffusion-weighted imaging to distinguish well-differentiated hepatocellular carcinomas from benign nodules in patients with chronic liver disease. *AJR* 2011; 197:[web]W868–W875
14. European Association for the Study of the Liver. EASL clinical practice guidelines: management of hepatocellular carcinoma. *J Hepatol* 2018; 69:182–236
15. Sica GT. Bias in research studies. *Radiology* 2006; 238:780–789
16. von Elm E, Altman DG, Egger M, Pocock SJ, Gøtzsche PC, Vandenbroucke JP; STROBE Initiative. The Strengthening the Reporting of Observational Studies in Epidemiology (STROBE) statement: guidelines for reporting observational studies. *J Clin Epidemiol* 2008; 61:344–349
17. Child CG, Turcotte JG. Surgery and portal hypertension. In: Child CG, ed. *The liver and portal hypertension*. Philadelphia, PA: Saunders, 1964:50–64
18. Pugh RN, Murray-Lyon IM, Dawson JL, Pietroni MC, Williams R. Transection of the esophagus in bleeding oesophageal varices. *Br J Surg* 1973; 60:648–652
19. Kim WR, Biggins SW, Kremers WK, et al. Hyponatremia and mortality among patients on the liver-transplant waiting list. *N Engl J Med* 2008; 359:1018–1026
20. Hiraoka A, Kumada T, Kudo M, et al.; Real-Life Practice Experts for HCC (RELPEC) Study Group and HCC 48 Group (hepatocellular carcinoma experts from 48 clinics). Albumin-bilirubin (ALBI) grade as part of the evidence-based clinical practice guideline for HCC of the Japan Society of Hepatology: a comparison with the liver damage and Child-Pugh classifications. *Liver Cancer* 2017; 6:204–215
21. Kambadakone AR, Fung A, Gupta RT, et al. LI-RADS technical requirements for CT, MRI, and contrast-enhanced ultrasound. *Abdom Radiol (NY)* 2018; 43:56–74
22. Bashir MR, Gupta RT, Davenport MS, et al. Hepatocellular carcinoma in a North American population: does hepatobiliary MR imaging with Gd-EOB-DTPA improve sensitivity and confidence for diagnosis? *J Magn Reson Imaging* 2013; 37:398–406
23. Pietryga JA, Burke LM, Marin D, Jaffe TA, Bashir MR. Respiratory motion artifact affecting hepatic arterial phase imaging with gadoxetate disodium: examination recovery with a multiple arterial phase acquisition. *Radiology* 2014; 271:426–434
24. Cerny M, Bergeron C, Billiard JS, et al. LI-RADS for MR imaging diagnosis of hepatocellular carcinoma: performance of major and ancillary features. *Radiology* 2018; 288:118–128
25. American College of Radiology website. New: CT/MRI CT/MRI LI-RADS® v2018. www.acr.org/Clinical-Resources/Reporting-and-Data-Systems/LI-RADS/CT-MRI-LI-RADS-v2018. Accessed July 28, 2018
26. Rimola J, Forner A, Tremosini S, et al. Non-invasive diagnosis of hepatocellular carcinoma ≤ 2 cm in cirrhosis: diagnostic accuracy assessing fat, capsule and signal intensity at dynamic MRI. *J Hepatol* 2012; 56:1317–1323
27. Khan AS, Hussain HK, Johnson TD, Weadock WJ, Pelletier SJ, Marrero JA. Value of delayed hypointensity and delayed enhancing rim in magnetic resonance imaging diagnosis of small hepatocellular carcinoma in the cirrhotic liver. *J Magn Reson Imaging* 2010; 32:360–366
28. Cerny M, Chernyak V, Olivié D, et al. LI-RADS version 2018 ancillary features at MRI. *RadioGraphics* 2018; 38:1973–2001
29. Fowler KJ, Tang A, Santillan C, et al. Interreader reliability of LI-RADS version 2014 algorithm and imaging features for diagnosis of hepatocellular carcinoma: a large international multireader study. *Radiology* 2018; 286:173–185
30. Iannaccone R, Laghi A, Catalano C, et al. Hepatocellular carcinoma: role of unenhanced and delayed phase multi-detector row helical CT in patients with cirrhosis. *Radiology* 2005; 234:460–467

(Appendix starts on next page)

APPENDIX 1: Definitions of Major Imaging Features According to Liver Imaging Reporting and Data System (LI-RADS) Version 2017

Arterial Phase Hyperenhancement (Not Rim)

Nonrimlike enhancement in the arterial phase unequivocally greater in whole or in part than enhancement of liver. Enhancing part must have higher attenuation or intensity than liver in arterial phase.

Washout (Not Peripheral)

Nonperipheral visually assessed temporal reduction in enhancement in whole or in part relative to composite liver tissue from earlier to later phase resulting in hypoenhancement in the extracellular portion of the portal venous phase.

Enhancing Capsule

Smooth, uniform, sharp border around most or all of an observation, unequivocally thicker or more conspicuous than fibrotic tissue around background nodules, and visible as an enhancing rim in portal venous or transitional phase.

Size

Largest outer edge–to–outer edge dimension of an observation.

Threshold Growth

Size increase of a mass by a minimum of 5 mm and one of the following: 100% or greater increase in size in more than 6 months or previously unseen on CT or MRI, now 10 mm or larger in 24 months or less.

(Greater than 50% diameter increase in less than 6 months was not considered for threshold growth in this study, because lesions with arterial phase hyperenhancement and 50% or greater diameter increase in less than 6 months were categorized as LR-5g and therefore excluded.)

Reference Standard

The diagnosis of hepatocellular carcinoma (HCC) required one of the following conditions: pathologic proof of tumor presence obtained after liver transplant (n = 39), partial hepatectomy (n = 6), or biopsy (n = 19, 10 of which were obtained during laparoscopic ablation) or at autopsy (n = 1) *or* untreated lesion with conclusive LI-RADS version 2017 criteria for the diagnosis of HCC at follow-up contrast-enhanced CT (n = 4) or gadolinium-enhanced MRI (purely or prevalently extracellular contrast agent) (n = 40). The reference standard was considered inadequate if the lesion was treated before reaching the diagnosis of definitive HCC according to the reference standard. The median time between the initial imaging study and the diagnosis of HCC was 127 days (interquartile range, 48–189 days) for pathologic analysis and 199 days (range, 100–282 days) for imaging.

The diagnosis of malignancy other than HCC was made at pathologic analysis for three lesions in two patients, all three of which were combined HCC-cholangiocarcinoma at liver transplant. The diagnosis of malignancy was made at follow-up imaging for two lesions in one patient (metastases from neuroendocrine tumor at follow-up MRI). The diagnosis of neuroendocrine metastases was based on evidence at multiple follow-up MRI examinations (the last performed more than 6 years after index MRI) of an enlarging neuroendocrine tumor in the body of the pancreas and new multiple additional hepatic metastases that were identical to the primary pancreatic tumor.

The benign nature of other lesions was based on either pathologic proof at any time (n = 23) or stability or resolution at imaging follow-up with CT or MRI for a minimum of 24 months (n = 52). Among the 23 lesions proved benign at pathologic analysis, nine were macroregenerative nodules and one was an angiomyolipoma; finally, no malignancy was detected at pathologic analysis in the other 13 patients (i.e., liver transplant [n = 9], partial hepatectomy [n = 1], biopsy [n = 3]). In five of these 13 patients the benignancy of the lesion was also confirmed at follow-up MRI for a minimum of 24 months. Among the 52 lesions that were proved benign at follow-up imaging (51 with MRI, one with CT), 26 had resolved at follow-up, 23 were stable (one found to be benign focal fatty infiltration), one decreased in size, and two were ultimately found to be blood vessels.

FOR YOUR INFORMATION

The data supplement accompanying this web exclusive article can be viewed by clicking "Supplemental" at the top of the article.